RF MEMS Switches and Integrated Switching Circuits

A. Q. Liu, A. B. Yu, M. F. Karim, and M. Tang

Abstract— **Radio frequency (RF) microelectromechanical systems (MEMS) have been pursued for more than a decade as a solution of high-performance on-chip fixed, tunable and reconfigurable circuits. This paper reviews our research work on RF MEMS switches and switching circuits in the past five years. The research work first concentrates on the development of lateral DC-contact switches and capacitive shunt switches. Low insertion loss, high isolation and wide frequency band have been achieved for the two types of switches; then the switches have been integrated with transmission lines to achieve different switching circuits, such as single-pole-multi-throw (SPMT) switching circuits, tunable band-pass filter, tunable band-stop filter and reconfigurable filter circuits. Substrate transfer process and surface planarization process are used to fabricate the above mentioned devices and circuits. The advantages of these two fabrication processes provide great flexibility in developing different types of RF MEMS switches and circuits. The ultimate target is to produce more powerful and sophisticated wireless appliances operating in handsets, base stations, and satellites with low power consumption and cost.**

Index Terms—**Reconfigurable circuit, RF MEMS, Switch, SPMT, Tunable filter**

I. INTRODUCTION

RF MEMS switches can be fabricated in a number of ways using different micromachining processes. These processes have been extended to achieve three dimensional structures through bulk micromachining, in which large amounts of substrate are removed; and surface micromachining, in which layers are deposited on a surface followed by the removal of a sacrificial layer to release a moving structure. Even though some standard processes are current existed, they are not suitable for RF applications because of their resistive materials [1].

RF MEMS components that are currently under development in laboratories and industries around the world include switches, voltage-tunable capacitors, high quality factor (Q) micromachined inductors, film bulk acoustic resonators (FBAR) and MEMS resonators and filters [2]. Among them, the switches are the most fundamental devices, which can be used to form other RF MEMS circuits, such as tunable capacitors, tunable resonators and tunable filters.

Tunable filters are finding growing applications in many civil and military telecommunication/radar equipments such as electronic warfare, software programmable RF front-end and digital receivers. Common microwave tunable band-pass filters described in the literature can be classified into three basic categories: mechanically tunable, magnetically tunable, and electronically tunable filters [3]. The development of MEMS technology allows for the possibility of obtaining some desirable characteristics for tunable filters.

The objective of this paper is to review our research work on RF MEMS switches and switching circuits in the last five years. The organization of the paper is as follows. Fabrication process techniques are discussed in Section 2. Lateral DC-contact switches and capacitive shunt switches are discussed in Section 3. Section 4 presents various switching circuits.

II. FABRICATION PROCESS TECHNIQUES

Two different types of fabrication processes have

Manuscript received May 25, 2007; revised Aug. 20, 2007.
School of Electrical & Electronic Engineering, Nanyang Technological University Nanyang Avenue, Singapore 639798
E-mail: eaqliu@ntu.edu.sg

been developed to fabricate the above mentioned devices and circuits [4, 5]. First, bulk micromachining technology is developed based on deep etch of silicon and substrate transfer to glass technologies. Second, surface micromachining technology is developed based on thin film deposition and etching technologies. These two processes have their respective advantages. For instance, the bulk micromachining process is simple, where only one or two masks are needed. It allows for very precise control of device dimensions with high reliability. The surface micromachining process, on the other hand, deposits and patterns different metal and dielectric layer with different thickness and hence is more suitable for the fabrication of the capacitive switches and the circuits based on the capacitive switches. The advantages of these two fabrication processes allow greater flexibility in developing different types of RF MEMS switches, and integrate the switches into the switching circuits eventually.

1. Substrate Transfer Technique

Fig. 1 shows a wafer transfer fabrication process that specially developed for lateral DC-contact switches and switching circuits [6-8]. The fabrication process begins with the deposition and patterning of a 2-μm-thick plasma-enhanced chemical vapor deposition (PECVD) silicon dioxide (SiO_2). Then, 50-70 μm thick high-aspect-ratio silicon structures are etched in a silicon wafer via deep reactive ion etching (DRIE) process using SiO_2 as the hard mask. After removal of the PECVD SiO_2 using reactive ion etching (RIE) process, a 2000-Å-thick thermal SiO_2 is grown to cover everywhere of the silicon structures (Fig. 1 (a)). After that, the silicon wafer is bonded to a 500-μm-thick glass (Pyrex 7740) wafer using anodic bonding technique (Fig. 1 (b)). Next, the silicon wafer is thinned from the backside in two steps. First, grinding and polishing are used to thin silicon rapidly until the deepest trenches are exposed (Fig. 1 (c)). Second, 30% aqueous solution of potassium hydroxide (KOH) at 40 °C is used to etch the silicon until all silicon structures are exposed to the air (Fig. 1 (d)). The thermal SiO_2 can protect the sidewalls of the exposed silicon structures from the erosion of the KOH solution. After the removal of the exposed thermal SiO_2 in the buffered oxide etchant (BOE), the wafer stack is dipped in the aqueous solution of hydrofluoric acid (HF)

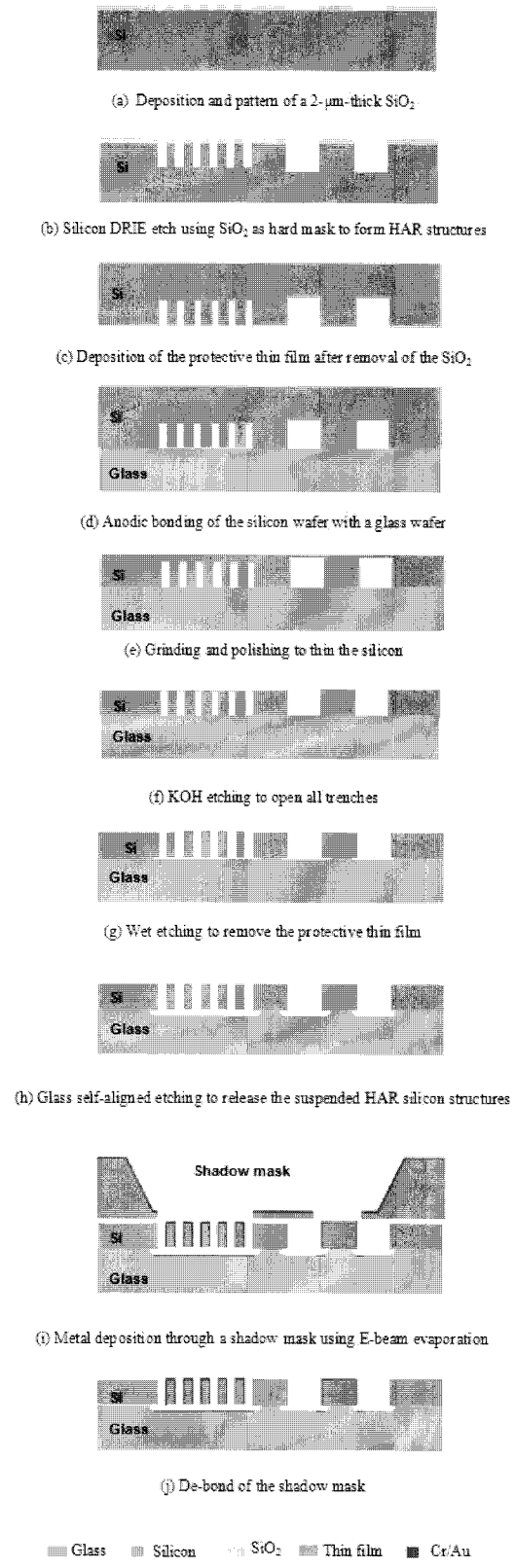

Fig. 1. Schematic of the fabrication process flow.

for 30 minutes to etch the glass and release the high-aspect-ratio suspended structures (Fig. 1 (e)). The silicon

structures serve as the hard mask for the glass etching. Therefore, the glass etching is a self-aligned process and need no additional mask. At last, a thin layer of aluminum (Al) or chromium/ gold (Cr/ Au) is directly coated on the silicon structures using E-beam evaporation (Fig. 1 (f)). A cavity is formed in the glass due to the glass self-aligned etching. The vertical etching depth of the glass is 5.7 μm and the lateral etching width is 10.2 μm. A 1.2-μm-thick gold with 1000 Å chromium as adhesion layer is coated on the top surface and sidewalls of the silicon structure uniformly. Due to the step coverage of the evaporation, the gold coated on the sidewalls (0.45 μm) is thinner than the gold coated on the top surface (1.2 μm). On the sidewalls, the metal is tightly coated and is uniformly covering the height of the entire structures. This substrate transfer process has various advantages. First, high-aspect-ratio and deep silicon structures can be achieved since DRIE is conducted on the blank silicon wafer. These structures can produce large force for electrostatic actuators. Second, the silicon resistivity, the structure height, the glass thickness and the glass etch depth can be chosen with flexibility according to different applications. Third, the process provides low loss for RF applications when glass and high-resistivity silicon are chosen as the substrate and the device layer respectively. Fourth, the manufacturing cost is low since only one masks are needed in this process.

2. Surface Planarization Technique

Most of MEMS capacitive switches are fabricated using surface micromachining process where 5-9 masks are normally needed. Critical steps include low stress thin-film deposition for the metal bridge, surface roughness control for the capacitance area and fabrication of the flat metal bridge. Low stress thin film can be achieved by optimizing thin film deposition conditions, such as deposition gas pressure, power etc. The surface roughness of the capacitance area can be improved by using a refractory metal layer underneath the metal bridge [9]. Flat metal bridge can be obtained by planarizing the sacrificial layer underneath the metal bridge [10, 11].

Surface planarization can greatly improve the RF performance of the capacitive switch. Spin coating a layer of photoresist to fill in the slot of coplanar

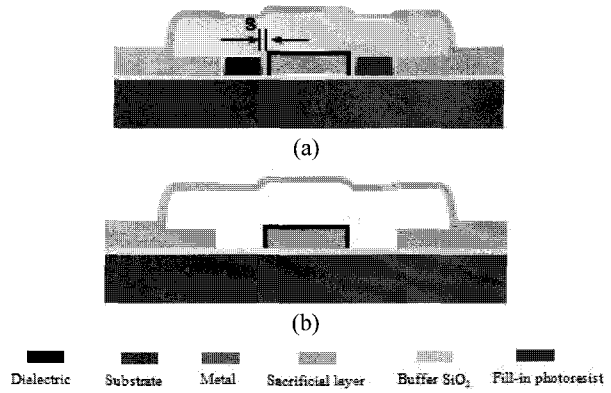

Fig. 2. Cross section views of the capacitive switch. (a) before photoresist removal; (b) after photoresist removal

waveguide (CPW) line is one of the methods to planarize the sacrificial layer [10]. This is shown in Fig. 2. The thickness of the photoresist that filled-in the slot is equal to the thickness of the CPW line. If the sacrificial layer is also photoresist, in order to avoid peeling-off of the photoresist that filled-in the slot of the CPW line, the hard-bake temperature, Tf, for the planarization step should be about 30 °C higher than the hard-bake temperature, Ts, for the sacrificial photoresist patterning step. Another factor that has to be taken into consideration is the masks alignment and tolerance control in the fabrication process. The optimal gap spacing (s) between the patterned fill-in photoresist and the CPW line, as indicated in Fig. 2(a), is 3 μm. For this spacing the masks alignment mismatch will not affect the patterns of the fill-in photoresist.

III. RF SWITCHES

RF MEMS switches are the most important and the earliest developed RF MEMS components. Up to date, various research work has been conducted on different types of RF MEMS switches. It is seen that in the last two decades a lot of work was accomplished, including RF characteristics, mechanical characteristics, fabrication issues, power handling, reliability and even package etc.

The RF MEMS switches can be categorized according to four characteristics: (1) RF circuit configuration; (2) mechanical structure; (3) form of contact and (4) method of actuation. Among these DC-contact switches and capacitive switches are the most frequently reported switches.

1. DC-contact Switches

DC-contact switches use metal to metal direct contact to achieve an ohmic contact between a signal line and a contact beam. This ohmic contact characteristic makes the device suitable for wide band applications, including DC, as well as high frequencies. Both surface and bulk micromachining processes are used to fabricate the DC-contact switch. In this paper, however, only the DC-contact switches fabricated using bulk micromachining process are discussed.

Fig. 3 shows a DC-contact lateral series switch that is fabricated using the substrate transfer process [12]. A high-aspect-ratio cantilever beam with beam-mass structure is employed as a lateral actuator. With a DC bias added between the ground and the cantilever beam, electrostatic force pushes the cantilever beam to move laterally and contact the signal line.

Fig. 4 presents the measured RF performance of the switch. The measurements show that the optimized lateral switch has low insertion loss (< 1 dB), high return loss and isolation (> 20dB) from 50 MHz to 25 GHz. The threshold voltage is less than 25 V. Fig. 5 shows the experimental result of switching speed that is 35 μs of switching-on time and 36 μs of switching-off time.

As the lateral DC-contact switch is based on high aspect ratio structure, the Si-core CPW transmission line is also fabricated and characterized. Fig. 6 gives the measurement results. The experimental results also verify that the Si-core CPW supports quasi-TEM mode propagation up to 25 GHz with attenuation of less than 4 dB/cm. It is found that the conductor loss dominates the attenuation of the Si-core CPW. To achieve the low-loss Si-core CPW, some useful guidelines are suggested. These include (1) depositing sufficiently thick metal and improving the step coverage of the metal deposition; (2) utilizing low loss substrate, such as glass; and (3) using high resistivity silicon as core material.

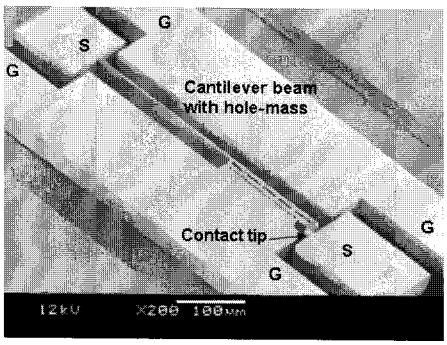

Fig. 3. SEM micrograph of a lateral switch with the hole-mass (G: ground, S: signal).

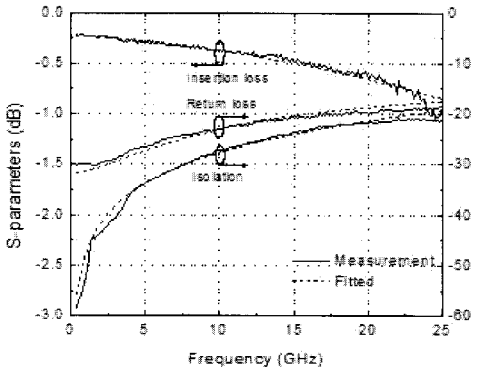

Fig. 4. Comparison between measured and fitted S-parameters of the lateral switch.

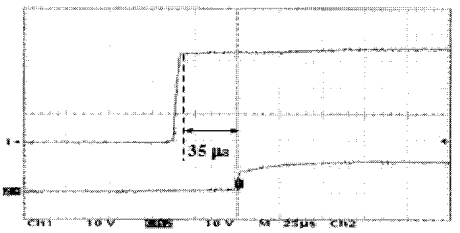

(a)

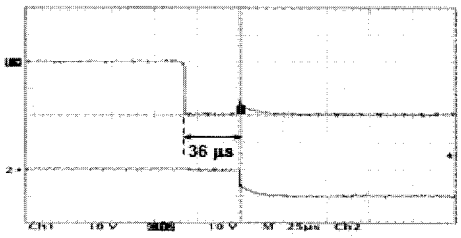

(b)

Fig. 5. Experimental results of switching performance of a lateral switch (a) close-state; (b) open-state.

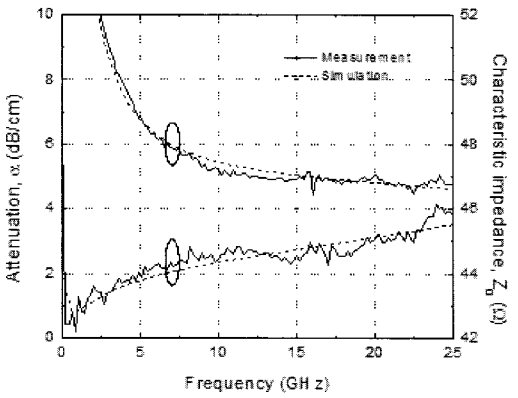

Fig. 6. Comparison of the measurement and the simulation results of a HRSi-core CPW on a glass substrate (T = 62 μm, h_r ≈ 6 μm, w_r ≈ 10 μm and 1-μm-thick Au coating).

The advantages of the lateral DC-contact switches are high fabrication yield, low costs, high stability and reliability. The long-term reliability is dependent on the

hard contact materials, large contact area and hermetic package [13]. The lateral DC-contact switch can be easily integrated into the switching matrix.

2. Capacitive Switches

Capacitive switches are key elements in various applications such as tunable capacitors and tunable filters. Normally, the capacitive switches are fabricated only using surface micromachining process because it is difficult to implement a thin dielectric layer between a movable beam and a signal line for the bulk micromachining process.

An important figure of merit of the RF MEMS capacitive switch is the ratio of down-state capacitance to up-state capacitance. Broader frequency band can be achieved with larger capacitance ratio. However, the actual capacitance ratio is always smaller than the designed value because of the down-state capacitance degradation problem. This down-state capacitance degradation problem is usually a result of nonplanarization of metal bridge, surface roughness of capacitance area and etching hole in the metal bridge. [10, 11].

Fig. 7 shows two capacitive shunt switches that are fabricated using the surface micromachining process. Fig.

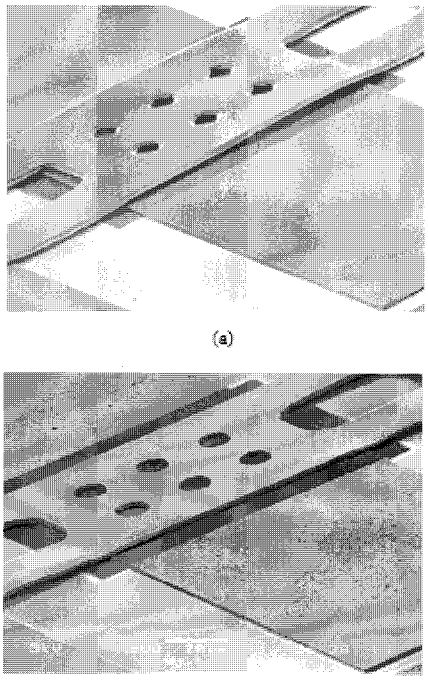

(a)

(b)

Fig. 7. SEM photos of the capacitive shunt switch. (a) Switch A, without fill-in photoresist and (b) Switch B, with fill-in photoresist.

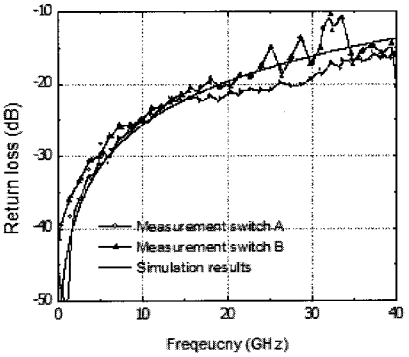

(a)

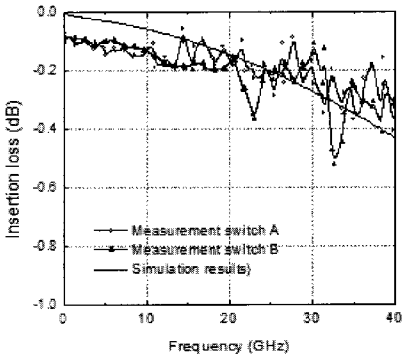

(b)

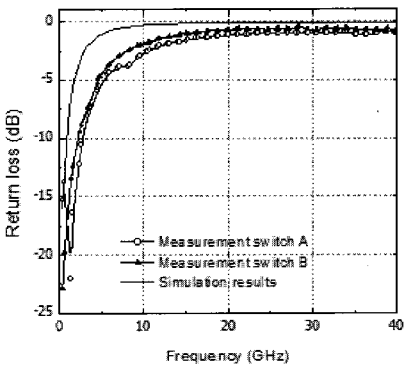

(c)

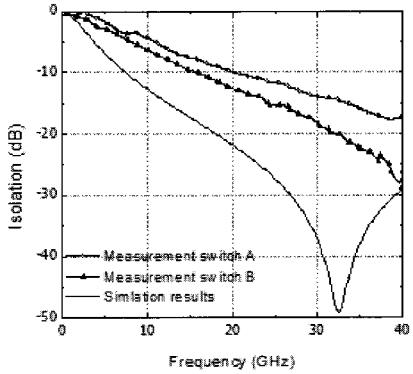

(d)

Fig.8. Comparison of simulated and measured S-parameters. (a) up-state return loss; (b) up-state insertion loss; (c) down-state return loss; and (d) down-state isolation.

7(a) (Switch A) is fabricated without planarization and Fig. 7(b) (Switch B) is fabricated with planarization. Fig. 8 shows the simulation and measurement results for Switch A and Switch B. The simulations in Fig. 8 are conducted using Ansoft's high frequency simulation software (HFSS) and assuming that the entire bridge area above the CPW center conductor contacts the dielectric layer when the bridge is pulled down. Figs. 8 (a) and (b) show that the up-state performances of Switch A and Switch B are similar. Both are comparable to the simulation results. Figs. 8 (c) and (d) show that at the down-state, the isolation of Switch B is 2.2 dB higher at 15 GHz and 10 dB higher at 40 GHz compared to that of Switch A. The results indicate that after surface planarization, the contact area between the metal bridge and the dielectric layer increases.

Fig. 9 shows the effects of surface roughness on the performance of the switch. Different metal materials are used underneath the dielectric layer for these switches. These different metal materials give different surface roughness of the capacitance area during the process. For 0.5 μm thick of Ti, Cr, Al and Cu thin film, the surface roughness of the capacitance area are 2.2 nm, 4.5

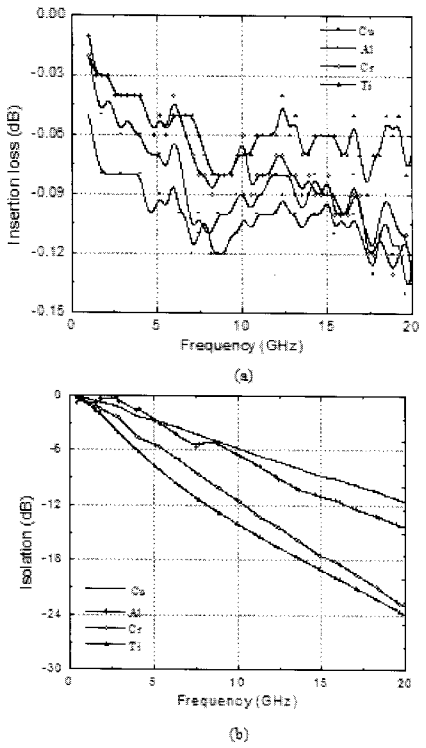

Fig. 9. Measurement results of RF properties versus different metal materials (a) insertion loss; (b) isolation (with applied hold-down voltage of 30 *V*).

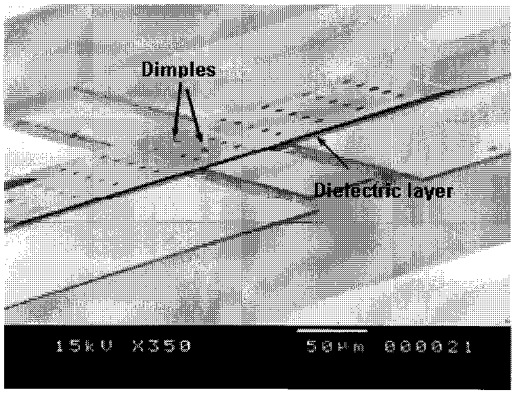

Fig. 10. SEM photo of DC-contact capacitive switch on low resistivity silicon substrate.

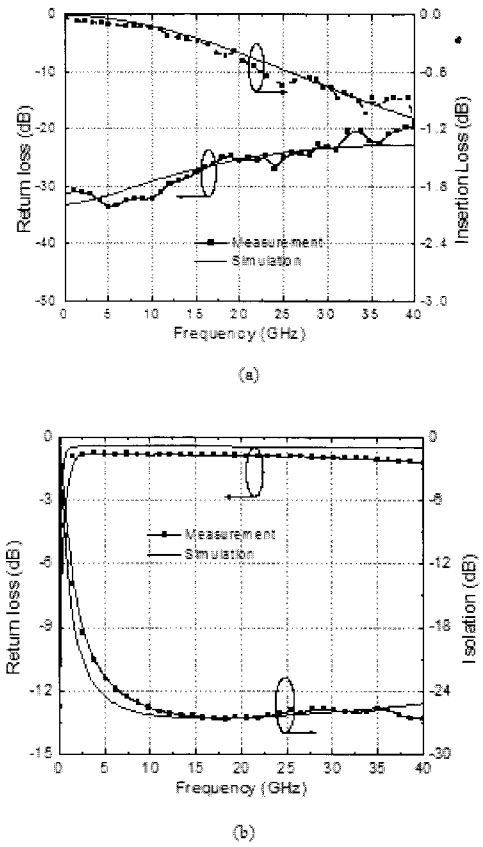

Fig. 11. Measurement and curve-fitted results (a) up-state; (b) down-state.

nm, 12.3 nm and 14.8 nm, respectively. From Fig. 9, the insertion loss increases and the isolation decreases with the increasing of the surface roughness of the capacitance area.

In order to avoid the down-state capacitance degradation and to achieve broadband capacitive switch, an innovated DC-contact capacitive shunt switch was developed [14]. In this design, the dielectric layer is shifted onto the grounds of a CPW transmission line, as shown in Fig. 10.

The switch is fabricated on low resistivity Si wafer with 18-μm-thick SiO_2 as isolation layer. The contact between the metal bridge and the center conductor becomes metal-metal contact after the metal bridge is driven down. The metal bridge, the dielectric layer and the grounds of the CPW transmission line consist of two metal-insulator-metal (MIM) capacitors in shunt.

Fig. 11 shows the measurement results of the DC-contact capacitive switch. The insertion loss of the switch is lower than 1.2 dB up to 40 GHz. The extracted up-state capacitance is 30 fF. The isolation of the switch is 13 dB at 1 GHz, 26 dB at 20 GHz and 27 dB at 40 GHz. The capacitance ratio of the DC-contact capacitive switch is 1000.

The advantages of the capacitive switch are more flexible to construct tunable or reconfigurable switching circuits. The long term reliability of the capacitive switches is mainly limited by dielectric charging and can be improved by using high quality dielectric layer, proper design of the metal bridge and bipolar driving voltage [15].

IV. Reconfigurable Switching Circuits

1. Single-Pole-Multi-Throw Switching Circuits

By directly applying the Si-core CPW and lateral switches, SPMT switching circuits are designed, fabricated and measured [6, 8, 16]. Fig. 12 shows a SEM photo of a SPDT switching circuit. A SPST switch is located on each of the output lines of a T-junction. The two laterally moving switches are arranged parallel to each other. A Si-core metal-coated CPW is used as a transmission line,. The two cantilever beams share a common ground line

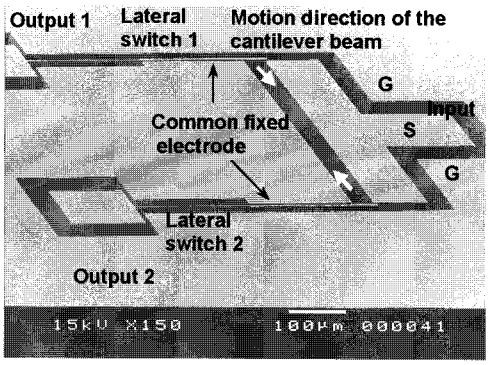

Fig. 12. some words is not clear. We have changed the figure as follow.

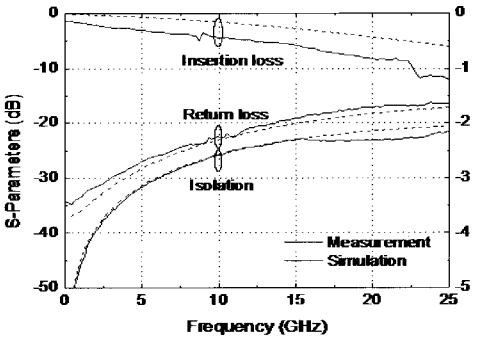

Fig. 13. Measured and fitted results of the in-line SPDT switching circuit.

and a common fixed electrode. The signal can therefore be routed to the different output port with one switch at the open-state and the other at the close-state. Bond wires are applied to electrically connect the different ground conductors to suppress parasitic, non-balanced modes effectively, especially at high frequencies range.

The measured S-parameters of the SPDT switching circuit with bond wires are shown in Fig. 13. The bias voltage of 30 V is applied from the output port to close the corresponding switch. The insertion loss is less than 1 dB up to 22 GHz. The return loss is higher than 17 dB and the isolation is higher than 25 dB up to 25 GHz.

2. Tunable Band-Pass Filter

Fig. 14 is a SEM photo of a two-pole tunable band-pass filter [17]. The filter is Chebyshev type and consists of two LC resonators, three series coupling capacitors and six DC-contact shunt switches. In each resonator, the shunt capacitors are realized by implementing shunt metal bridges 2 μm above the center conductor of the CPW transmission line whereas the shunt inductors are realized by the shunt shorted-end stub. The three series coupling capacitors are realized by three MIM capacitors with 1-μm- thick SiO_2 as dielectric material. The tuning approach is to change the length of the shunt shorted-end stubs with DC-contact switch. In this tuning approach, only shunt the inductors is tuned in each resonator sub-circuit. The measurement results in Fig. 15 show that the central frequency of the tunable band-pass filter can be shifted from 8 GHz to 11 GHz (37 % tuning range). The 3 dB bandwidth is 10 % in the whole tuning range. The insertion loss in the passband is varied between 5.5 dB to 7.5 dB and the return loss in the pass-band is higher than 10 dB. The advantage of this tuning approach is wide tuning range with few tuning elements.

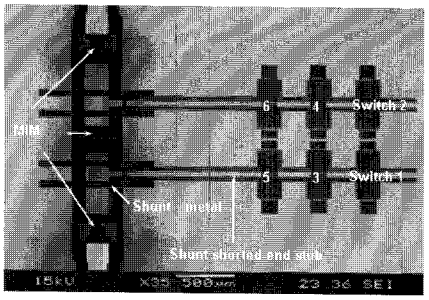

Fig. 14. SEM micro-photo of two-pole tunable band-pass filter.

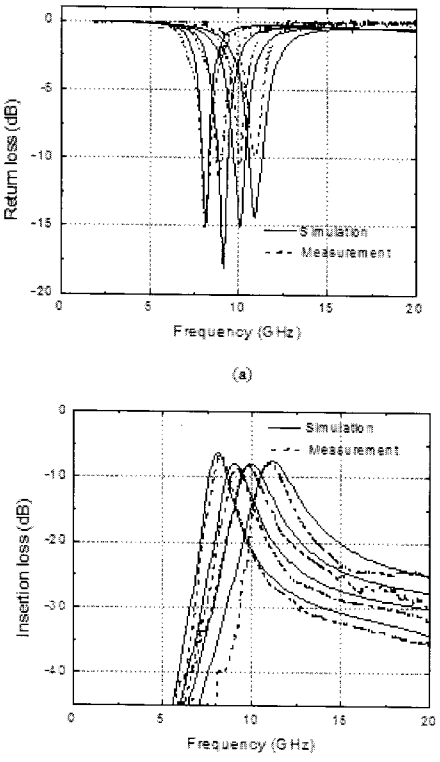

Fig. 15. Measured frequency response of the tunable band-pass filter (a) Reflection; (b) Insertion loss.

3. Tunable Band-Stop Filter

Besides the tunable band-pass filter, tunable band-stop filter can also be realized using MEMS technology [18, 19]. Fig. 16 shows such a tunable band-stop filter. The filter consists of two groups of MEMS bridges and three unit electromagnetic bandgap (EBG) cells that series connected together. The MEMS bridges act as tuning elements by change the height of the bridges, i.e. varying the capacitance, when DC bias voltage is applied between the signal line and the ground plane. An equivalent LC circuit is used to describe the tunable EBG structure as shown in Fig. 17. The lumped capacitance, C1, is basically due to the transverse slot on the ground, while the inductance,

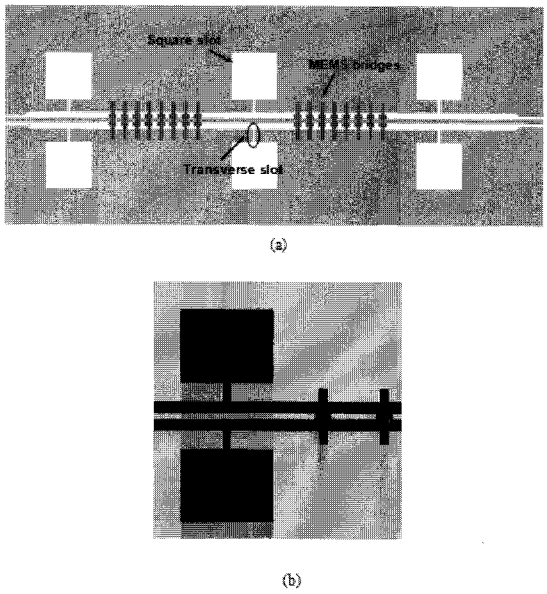

Fig. 16. (a) Schematic drawing of tunable band-stop filter; (b) SEM photo of part of tunable band-stop filter.

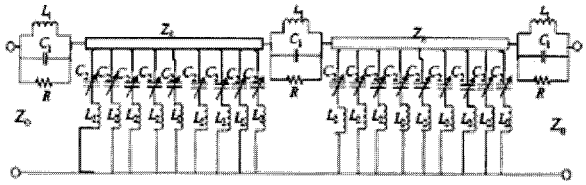

Fig. 17. Equivalent parallel resonant circuit for the tunable band-stop filter.

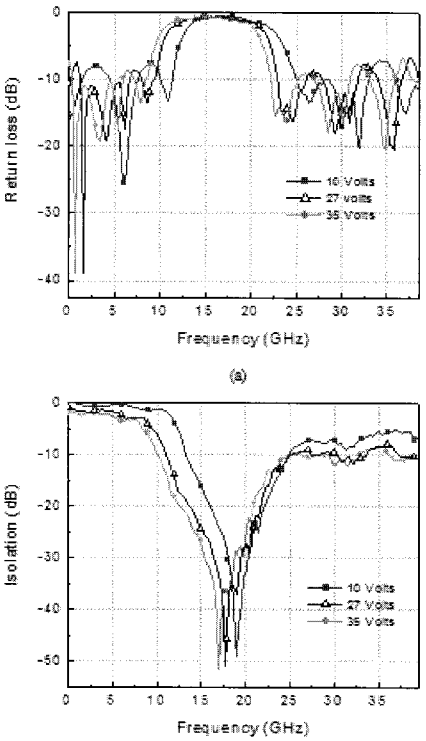

Fig. 18. Measurement results of the MEMS tunable band-stop filter (a) Return loss; and (b) Isolation.

L1, is related to the magnetic flux passing through the aperture on the ground. Since MEMS bridges are shunt capacitive, so they can be modeled as an equivalent parallel capacitor, C2, and inductor, L2, in each resonator section. Fig. 18 gives the measurement results. The measurement results of the tunable band-stop filter show that the tuning range is from 19 GHz to 17.3 GHz. The insertion loss varies from 0.7 dB to 2.2 dB.

4. Reconfigurable Filter

Reconfigurable circuit is one of the important areas that MEMS technology can have significant impact [20-22]. Fig. 19 shows a SEM photo of a micromachined switching reconfigurable filter. It is designed based on a EBG structure. Each unit of EBG cell consists of a small square slot and a large square slot. The two square slots are connected by a transverse slot (2nd transverse slot in Fig. 19). There is a DC-contact above each 2nd transverse slot. Fig. 20 shows the equivalent circuit for the filter. The lumped capacitances, C1 and C2, are contributed by the 1st and the 2nd transverse slot; whereas the inductances, L1 and L2, are related to the magnetic flux passing through the two square slots, respectively. Fig. 21 shows the measurement results. When the DC-contact switches are at off-state (up-state), all the square slots and the transverse slots have effect on the RF signal distribution, which means all the capacitances (C1 and C2) and the inductances (L1 and L2) in Fig. 20 are connected to the circuit. The resulted frequency response of the whole circuit shows bandpass characteristic, as GHz and the out-of-band rejection is greater than 20 dB. The 3-dB bandwidth is 9.2 GHz. When the DC-contact switches are at on-state (down-state), the large square slot and the 2nd transverse slot are shorted, which indicates the the capacitance C2 and the inductance L2 are excluded in the circuit. As a result, the whole circuit

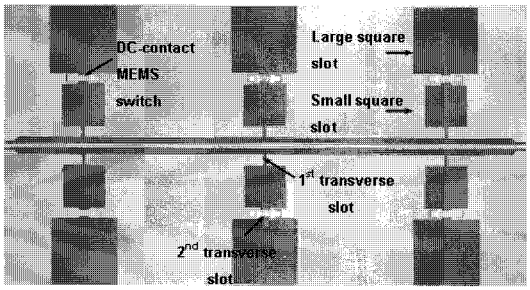

Fig. 19. SEM photo of the reconfigurable filter.

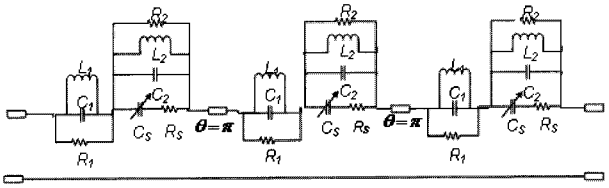

Fig. 20. Equivalent circuit of the reconfigurable filter.

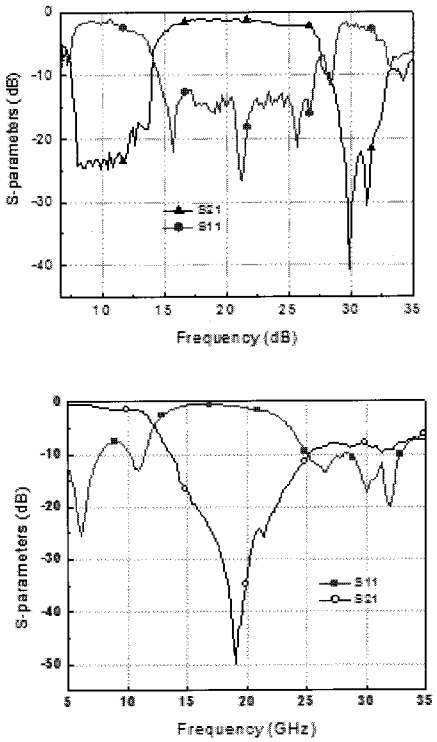

Fig. 21. Measurement results of the reconfigurable filter using MEMS switches (a) off-state of switch, band-pass filter and (b) on-state of switch, band-stop filter.

becomes a band-stop filter with the center frequency of 19.8 GHz, as shown in Fig. 21(b). The 20 dB rejection bandwidth is from 17 to 22.5 GHz.

V. Conclusions

The recent progress in RF MEMS is reviewed in this paper. Devices that are reviewed include lateral metal contact switch, capacitive shunt switches, SPMT switching circuits, tunable filters and reconfigurable filter. The lateral contact metals switches shows enhanced performance in terms of lower insertion loss of 1 dB at 25 GHz. In capacitive shunt switches, the down-state capacitance degradation is analyzed and a novel DC-contact capacitive switch is designed, fabricated and characterized. The isolation of this innovated DC-contact capacitive switch is higher than 13 dB from 1 GHz to 40 GHz. Besides

single switch components, different applications of the switches are described. The lateral DC-contact switch is implemented to form the SPMT switching circuits with insertion loss of 1 dB up to 20 GHz. The capacitive switch is used as tuning element to achieve tunable band-stop filter with the tuning range from 19 GHz to 17.3 GHz. Besides, an inductive tuning band-pass filter with tuning range from 8 GHz to 11 GHz and a reconfigurable filter are also reported.

ACKNOWLEDGMENTS

The work is supported by the Research Grant from Defence Science & Technology Agency (DSTA) of Singapore.

REFERENCES

[1] A. S. Morris, S. Cunningham, D. Pereus and G. Schropfer, "High-performance integrated RF-MEMS: Part 1 – the process," *11th GaAs Symposium*, Munich 2003 pp. 325 – 328

[2] H. A. C. Tilmans, W De Raedt and E. Beyne, "MEMS for wireless communications: 'from RF-MEMS components to RF-MEMS-SiP," *J. Micromech. Miroeng.* Vol. 13, 2003 pp. S139 – 163

[3] Y. H. Shu, J. A. Navaro and K. Chang, "Electronically switchable and tunable coplanar waveguide-slotline band-pass filters," *IEEE Trans. Microwave Theory Tech.*, Vol. 39, No. 3, March 1991 pp. 548-554

[4] J. Y. Park, G. H. Kim, K. W. Chung and J. U. Bu, "Monolithically integrated micromachined RF MEMS capacitive switches," *Sensors & Actuators A: Phys.* Vol. 89 2001 pp. 88-94

[5] E. J. J. Kruglick and K. S. J. Pister, "Lateral MEMS microcontact considerations," *IEEE J. Microelectromech. Systems*, Vol. 8, September 1999 pp. 264-271

[6] M. Tang, A. Q. Liu, and A. Agarwal, "A low-loss single-pole double-throw (SPDT) switch circuit," *The 14th International Conference on Solid-State Sensors, Actuators and Microsystems (Transducers '07)*, 10-14 June 2007, Lyon, France (accepted)

[7] M. Tang, A. Q. Liu, A. Agarwal and M. H. Habib, "A single-mask substrate transfer technique for fabrication of high-aspect-ratio micromachined structures," *J. Micromech. Microeng*, Vol. 17, No. 8, 2007 pp. 1575-1582

[8] M. Tang, A. Q. Liu, J. Oberhammer, "A silicon-on-glass single-pole double-throw (SPDT) switching circuit integrated with silicon-core metal-coated transmission line," *IEEE J. Microelectromech. Syst.*, (submitted)

[9] A. B. Yu, A. Q. Liu, Q. X. Zhang and H. M. Hosseini, "Effects of surface roughness on electromagnetic characteristics of capacitive switches," *J. Micromech. Miroeng.* Vol 16, 2006 pp. 2157-2166

[10] A. B. Yu, A. Q. Liu, Q. X. Zhang, A. Alphones, L. Zhu and S. A. Peter, "Improvement of isolation MEMS capacitive switch via membrane planarization," *Sensors and actuators A: Phys.* Vol. 119 2005 pp. 206 – 213

[11] A. B Yu, A Q Liu, J. Oberhammeh, Q. X. Zhang and H. M. Hosseini, "Characterization and optimization of dry releasing for the fabrication of RF MEMS capacitive switches," *J. Micromech. Microeng*, Vol. 17, No. 10 2007 pp. 2024-2030

[12] A. Q. Liu, M. Tang, A. Agarwal, and A. Alphones, "Low-loss lateral micromachined switches with frequencies from DC to 25 GHz," *J. Micromech. Miroeng.*, Vol. 15, No. 1, 2005 pp. 157-167

[13] J. Schimkat, "Contact materials for microrelays," *11th IEEE International Conference on Microelectromechanical Systems*, Heidelberg, Germany, 1998, pp. 190-194

[14] A. B. Yu, A. Q. Liu, Q. X. Zhang and H. M. Hosseini, "Micromachined DC contact switch on low-resistivity silicon substrate," *Sensors & Actuators A* Vol. 127 February 2006 pp. 24-30

[15] X. B. Yuan, Z. Peng, James C. M. Hwang, D. Forehand and Charles L. Goldsmith, "Temperature acceleration of dielectric charging in RF MEMS capacitive switches," g effects on capacitive MEMS actuators," *IEEE MTT-S Int. Microwave Symp. Digest*, 11-16 June 2006, San francisco, USA, pp. 47-50

[16] M. Tang, W. Palei, W. L. Goh, A. Agarwal, L. C. Law and A. Q. Liu, "A single pole double throw (SPDT) circuit using lateral metal contact

micromachined switches," *IEEE MTT-S Int. Microwave Symp. Digest*, 8-12 June 2004, Boston, USA, pp. 581-584

[17] A. B. Yu, A. Q. Liu , and Q. X. Zhang, "Wide tuning range MEMS band-pass filter with inductance change," *The 13th International Conference on Solid-State Sensors, Actuators and Microsystems (Transducers '05)*, 5-9 June, 2005, Seoul, Korea, Vol 2, pp. 2061-2064

[18] M. F. Karim, A. Q. Liu, A. Alphones and A. B. Yu, "A tunable bandstop filter via the capacitance change of micromachined switches," *J. Micromech. Microeng*, Vol. 16, No. 4, pp. 851-861, 2006

[19] X. J. Zhang, A. Q. Liu, M. F. Karim, A. B. Yu, Z. X. Shen, "MEMS based photonic bandgap (PBG) bandstop filter," *IEEE MTT-S Int. Microwave Symp. Digest*, 8-12 June 2004, Boston, USA, pp. 1463-1466

[20] M. F. Karim, A. Q. Liu, A. B. Yu, and A. Alphones, "Miniaturized Bandpass Filter for Broad-Band Applications, *IEE Electronics Letters*, (submitted)

[21] M. F. Karim, A. Q. Liu, A. Alphones and A. B. Yu, "A novel reconfigurable filter using periodic structures," *IEEE MTT-S Int. Microwave Symp. Digest*, 11-16 June, 2006, San Francisco, USA pp. 943-946.

[22] M. F. Karim, A. Q. Liu, A. Alphones, and A. B. Yu, "A reconfigurable micromachined switching filter using periodic structures," *IEEE Transaction on Microwave Theory & Tech.*, Vol. 55, No. 6 June 2007 pp. 1154-1162

A. Q. Liu (Ai-Qun Liu) received his PhD degree from National University of Singapore (NUS) in 1994. His MSc degree was received from Beijing University of Posts & Telecommunications in 1988, and BEng degree was received from Xi'an Jiaotong University in 1982. Currently, he is an Associate Professor at School of Electrical & Electronic Engineering, Nanyang Technological University (NTU). He is as an Associate Editor for the IEEE Sensor Journal and also a Guest Editor for Sensors & Actuators A Physical. His research interests are MEMS design, simulation and fabrication processes.

A. B. Yu received the B.Eng. degree in materials science and the M. Eng. degree in electronic materials and devices from Shanghai Jiaotong University, Shanghai, China, in 1993 and 1996, respectively, and is working toward the Ph.D. degree at Nanyang Technological University. Currently he is a Research Engineer with the Lab of Microsystems, Modules and Components, Institute of Microelectronics, Singapore. His research interests include MEMS design, fabrication and packaging process.

M. F. Karim received the B.Eng. degree from the National University of Science and Technology, Raealpindi, Pakistan, in 2000, the Masters of Science degree from Nanyang Technological University, Singapore, in 2002, and is currently working toward the Ph.D. degree at Nanyang Technological University. His research interests include RF MEMS, antennas, and EBG structures.

M. Tang received the B.Eng. degree in Applied Chemistry and MSc degree in Microelectronics and Solid-state Electronics from Shanghai Jiao Tong University in 1998 and 2001, respectively. Then, she received her PhD degree in MEMS and Microelectronics at Nanyang Technological University in 2007. Currently she is a Senior Research Engineer with the MEMS program, Institute of Microelectronics, Singapore. Her research interests include MEMS design and fabrication process.